Geophysical Research Letters

RESEARCH LETTER
10.1029/2022GL101235

Midwinter Dry Spells Amplify Post-Fire Snowpack Decline

Benjamin J. Hatchett[1], Arielle L. Koshkin[1,2], Kristen Guirguis[3], Karl Rittger[4], Anne W. Nolin[2], Anne Heggli[1], Alan M. Rhoades[5], Amy E. East[6], Erica R. Siirila-Woodburn[5], W. Tyler Brandt[3], Alexander Gershunov[3], and Kayden Haleakala[3,7]

[1]Division of Atmospheric Sciences, Desert Research Institute, Reno, NV, USA, [2]Department of Geography, University of Nevada, Reno, NV, USA, [3]Climate, Atmospheric Science and Physical Oceanography Division, Scripps Institution of Oceanography, University of California San Diego, La Jolla, CA, USA, [4]Institute for Arctic and Alpine Research, University of Colorado, Boulder, CO, USA, [5]Earth and Environmental Sciences Area, Lawrence Berkeley National Laboratory, Berkeley, CA, USA, [6]U.S. Geological Survey, Santa Cruz, CA, USA, [7]Department of Civil and Environmental Engineering, University of California, Los Angeles, Los Angeles, CA, USA

Abstract Increasing wildfire and declining snowpacks in mountain regions threaten water availability. We combine satellite-based fire detections with snow seasonality classifications to examine fire activity in California's seasonal and ephemeral snow zones. We find a nearly tenfold increase in fire activity during 2020–2021 versus 2001–2019. Accumulation season broadband snow albedo declined 25%–71% at two burned sites (2021 and 2022) according to in-situ data relative to un-burned conditions, with greater declines associated with increased burn severity. By enhancing snowpack susceptibility to melt, both decreased snow albedo and canopy drove midwinter melt during a multi-week dry spell in 2022. Despite similar meteorological conditions in December–February 2013 and 2022–linked to persistent high pressure weather regimes–minimal melt occurred in 2013. Post-fire snowpack differences are confirmed with satellite measurements. With growing geographical overlap between wildfire and snow, our findings suggest California's snowpack is increasingly vulnerable to the compounding effects of dry spells and wildfire.

Plain Language Summary Satellite fire detections indicate substantial increases in wildfire activity in California's snow-covered landscapes during 2020 and 2021, suggesting wildfire is increasingly altering mountain hydrology. During 2022, a multi-week mid-winter drought, or dry spell, occurred. A meteorologically-similar dry spell occurred in 2013, and the 2022 event provides a test case to examine how post-fire changes (canopy loss and deposition of burned dark material on snowpack) alter snowmelt patterns. Using field observations, weather station data, and satellite remote sensing of snow, we find large reductions in snow albedo and canopy cover drove rapid melt during the 2022 dry spell in burned areas whereas during 2013, minimal melt occurred. The societal connection between mountains and humans will be strained as mountains face increasing climate-related stressors. Midwinter drought, snow loss, and increasing wildfire are expectations of a warming world. Addressing these challenges requires innovative water and forest management paradigms. Our findings motivate additional research into assessing and planning for post-fire hydrologic changes in snow-dominated landscapes as both wildfire and dry spells will increase in frequency with climate warming.

Benjamin J. Hatchett and Arielle L. Koshkin contributed equally to this work.

Key Points:

- A 9.8x increase in satellite fire detections in California's snow zones in 2020–2021 versus 2001–2019 implies growing overlap in fire and snow
- Post-fire accumulation season broadband snow albedo declined 25%–71%, driving fewer snow-covered days and lower snow-cover fraction
- Compared with the meteorologically similar 2013 dry spell, albedo and canopy declines led to rapid midwinter melt in 2022

Supporting Information:

Supporting Information may be found in the online version of this article.

Correspondence to:

B. J. Hatchett,
benjamin.hatchett@dri.edu

Citation:

Hatchett, B. J., Koshkin, A. L., Guirguis, K., Rittger, K., Nolin, A. W., Heggli, A., et al. (2023). Midwinter dry spells amplify post-fire snowpack decline. *Geophysical Research Letters*, *50*, e2022GL101235. https://doi.org/10.1029/2022GL101235

Received 19 SEP 2022
Accepted 8 DEC 2022

1. Introduction

Communities and ecosystems worldwide rely on snowpacks to meet water demands (Immerzeel et al., 2020). A warming climate changes the spatial patterns and timing of snowpack accumulation and melt by altering rain-snow partitioning, decreasing cold content and extending dry spell length (Gershunov et al., 2019; Lynn et al., 2020; Siirila-Woodburn et al., 2021). During the dry season, reduced snowpack combined with warming and drying enhances evaporative demand (Abatzoglou & Williams, 2016; Alizadeh et al., 2021) and lowers fuel moisture (McEvoy et al., 2019).

A warming, drying, and disturbance-prone climate combined with fire suppression and exclusion promotes severe wildfire at high elevations in the western U.S. (Millar & Stephenson, 2015). From 1984 to 2017, a 9% increase per year in area burned in the seasonal snow zone (Gleason et al., 2019) has been accompanied by a 7.6 myr^{-1} upslope increase in average wildfire elevation (Alizadeh et al., 2021). High burn severity areas also increased during these decades in the western U.S. (Parks & Abatzoglou, 2020).

Severe fires alter mountain snowpack processes near and below the treeline in two key ways. First, the decrease in forest canopy reduces interception of snowfall and increases incoming solar radiation. Every 20% increase in tree mortality increases below-canopy snow accumulation by 15% (Maxwell & Clair, 2019). Second, the black carbon deposited on the snow surface from standing burned vegetation reduces the snow albedo, which, combined with additional incoming solar radiation, accelerates snowmelt rates by up to 57% (Aubry-Wake et al., 2022; Gleason & Nolin, 2016; Gleason et al., 2013, 2019; Kaspari et al., 2015; Skiles et al., 2018).

Additional wildfire impacts on mountain hydrology include changes in soil hydraulic properties (Ebel & Moody, 2017), shifts in surface and subsurface water partitioning and flow pathways that increase water yields (Maina & Siirila-Woodburn, 2020), and forest structure (e.g., Moeser et al., 2020; Wilson et al., 2021). By altering the snow-vegetation-hydrology dynamics, severe fire in montane forests threatens ecosystems and the volume of snowpacks (Gleason et al., 2019; Siirila-Woodburn et al., 2021; Stevens, 2017). In the absence of fire, reduced canopy shifts the timing of peak snowpack later (Cristea et al., 2014). While it is well documented that spring snowmelt rates increase after wildfire (e.g., Gleason et al., 2019; Uecker et al., 2020), the mid-winter impacts remain understudied.

Our work is motivated by two recent phenomena adversely affecting California's snow hydrology: widespread severe wildfires of 2020–2021 reaching into the seasonal snow zone of mountain watersheds (Figure 1) and the multi-week, midwinter dry spell (hereafter MWDS) during the winter of 2022. We examine how the post-fire environment during the unusually dry conditions amplified snowmelt rates. We hypothesize that fire-impacted regions undergo declines in midwinter snow albedo that drive more rapid and earlier snowmelt compared with pre-fire or unburned conditions.

2. Methods

To assess impacts of MWDSs on post-fire environments, we examined data from three fires: The 2021 Caldor (89,773 ha; ignited 14 August) and Dixie Fires (389,837 ha; ignited 13 July) and the 2020 Creek Fire (153,738 ha; ignited 4 September) (Figure 2a).

2.1. Satellite Fire Detection in Seasonal and Ephemeral Snowpacks

Wildfire activity and outcomes are difficult to quantify (e.g., Andrews & Rothermel, 1982; Cheney, 1990; Justice et al., 2002; Keeley, 2009). Satellite-based fire detection is a useful proxy for generally assessing wildfire activity by providing consistent overflight return intervals across multiple years (Justice et al., 2002). We acquired daily fire detections at 1-km horizontal resolution from the MODerate resolution Imaging Spectroradiometer (MODIS) via the Fire Information for Response Management System database (https://firms.modaps.eosdis.nasa.gov) for the period spanning January 2001–December 2021. We subset all Californian fire detections into seasonal, ephemeral, and non-snow environments based on the concept of snow seasonality (Hatchett, 2021; Petersky & Harpold, 2018): the duration of time a landscape is continuously snow-covered. To assess seasonality, we applied the snow classifiers to a gridded, 4-km horizontal resolution, daily snow water equivalent (SWE) product (Broxton et al., 2019; Zeng et al., 2018) across California. Seasonal snowpacks are defined as grid cells with an annual median of at least 60 days of continuous snow cover spanning 1982–2018. Ephemeral snowpacks are defined as grid cells with intermittent (i.e., <60 days of continuous) snow cover.

2.2. Snow Remote Sensing

Daily observations of snow cover days, snow-covered fraction, and snow albedo in the Caldor Fire region are derived from Terra MODIS and are available from the Snow Today website (https://nsidc.org//snow-today). Initial estimates of snow surface properties are based on the MODIS Snow Covered Area and Grain size model (MODSCAG; Painter et al., 2009) and the MODIS Dust Radiative Forcing in Snow model (MODDRFS; Painter et al., 2012). Data from the two models are combined to create spatially and temporally complete (STC) daily images that account for forest canopy, off-nadir viewing, and cloud misidentification (Rittger et al., 2020). Snow cover errors from MODSCAG are half the size of standard MODIS products (Rittger et al., 2013) and albedo estimates from STC-MODSCAG/MODDRFS show 5% RMSE with no bias (Bair et al., 2019). STC-MODSCAG/MODDRFS data have been previously used for SWE reconstruction (Bair et al., 2016;

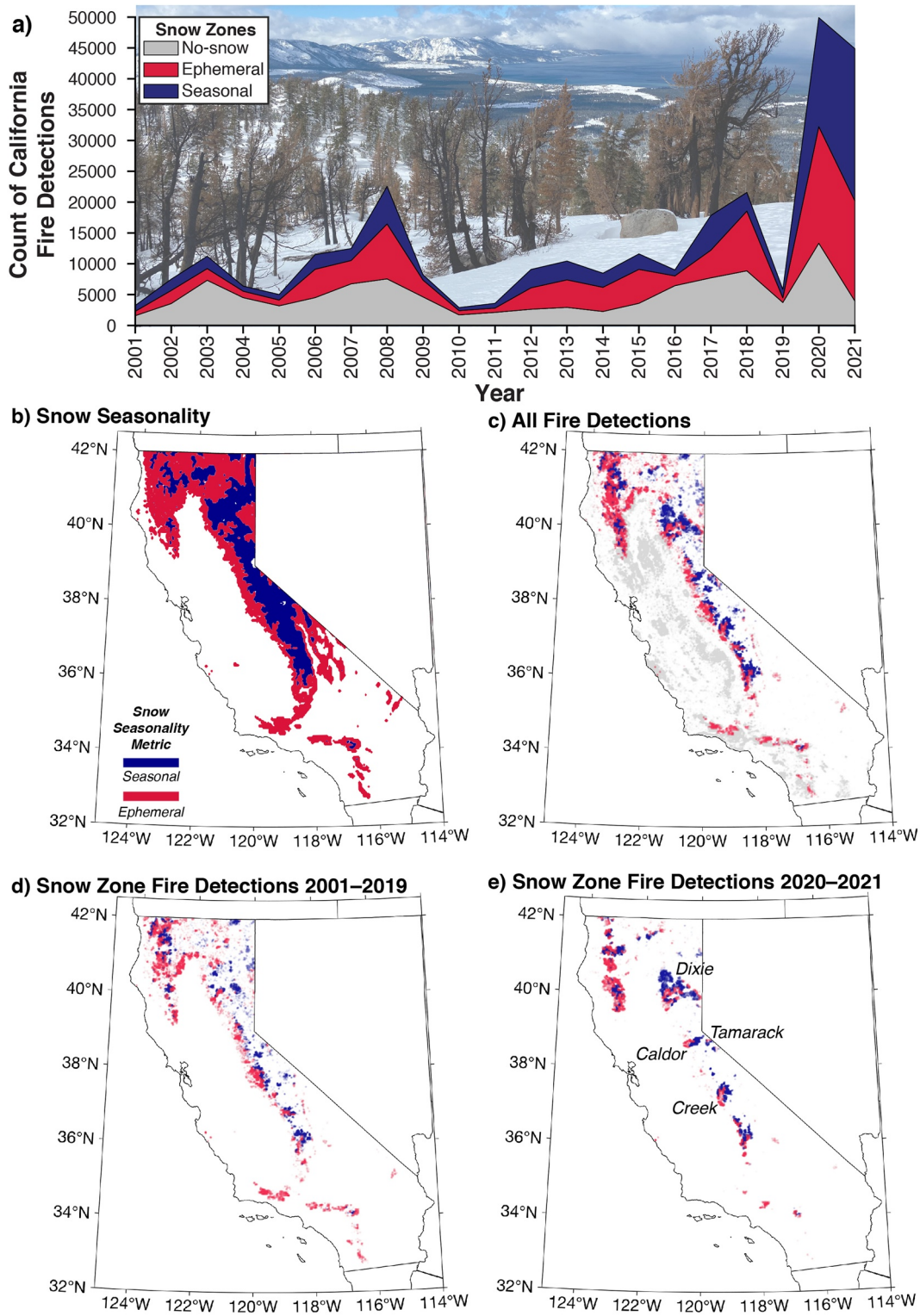

Figure 1. (a) Annual fire detections subset by snow seasonality (snow zone). (b) Snow seasonality classifications for California. (c) All fire detections (2001–2021), colored by snow seasonality classification: blue (seasonal), red (ephemeral), and gray (non-snow zone). Fire detections in seasonal (blue) and ephemeral (red) snow zones during (d) 2001–2019 and (e) 2020–2021, noting fires named in the text.

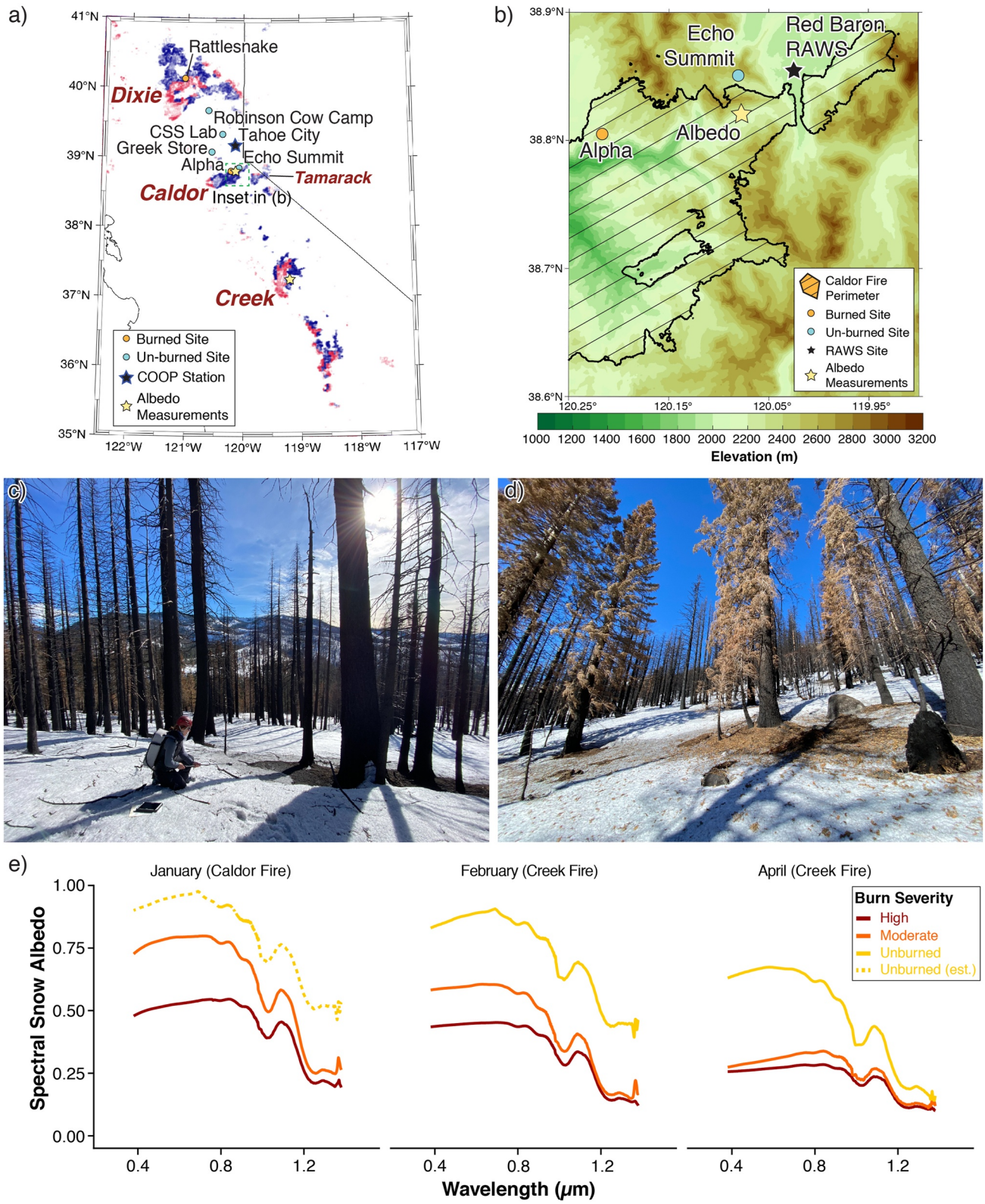
a)
Rattlesnake
Dixie
Robinson Cow Camp
CSS Lab
Tahoe City
Greek Store
Echo Summit
Alpha
Tamarack
Caldor
Inset in (b)
Creek
Burned Site
Un-burned Site
COOP Station
Albedo Measurements
41°N
40°N
39°N
38°N
37°N
36°N
35°N
122°W
121°W
120°W
119°W
118°W
117°W
b)
Echo Summit
Red Baron RAWS
Albedo
Alpha
Caldor Fire Perimeter
Burned Site
Un-burned Site
RAWS Site
Albedo Measurements
38.9°N
38.8°N
38.7°N
38.6°N
120.25°
120.15°
120.05°
119.95°
1000 1200 1400 1600 1800 2000 2200 2400 2600 2800 3000 3200
Elevation (m)
c)
d)
e)
January (Caldor Fire)
February (Creek Fire)
April (Creek Fire)
Burn Severity
High
Moderate
Unburned
Unburned (est.)
Spectral Snow Albedo
1.00
0.75
0.50
0.25
0.00
0.4
0.8
1.2
Wavelength (μm)

Figure 2.

Rittger et al., 2016), real-time estimates of SWE (Bair et al., 2018), estimating trends in snow cover at regional scales (Ackroyd et al., 2021), understanding snow darkening related to light-absorbing particles (LAP), (Huang et al., 2022; Sarangi et al., 2019, 2020) and improving snow albedo modeling (Hao et al., 2022).

2.3. In-Situ Albedo Measurements

We measured albedo in the Caldor Fire (measured once on 21 January 2022) and the Creek Fire (measured on 27–28 February and 1 April 2021; Figure 2a). Spectral albedo measurements were made using a Spectral Evolution RS-3500 Portable Spectroradiometer (RS-3500) equipped with a 180° field of view diffuser mounted on an extendable 1.2 m pole (Figure 2b). The RS-3500 has a spectral resolution of 1 nm over the spectral range 350–2500 nm. Measurements were made every 10 m along approximately flat terrain with one 100 m transect for each burn severity class (10 measurements per transect, with three observations, averaged together at each measurement point): high, moderate, and unburned. Soil burn severity for each fire was determined using maps produced by the U.S. Department of Agriculture Forest Service Burned Area Emergency Response (https://burn-severity.cr.usgs.gov/products/baer) using field-checked, remotely-sensed pre- and post-fire visible reflectances (Key & Benson, 2006).

2.4. Snowpack and Meteorological Observations

We used station-based observations of SWE, precipitation and solar radiation to examine the impacts of wildfire in burned and unburned areas in the Caldor and Dixie Fires. Daily SWE observations (1 October 2011–15 April 2022) spanned the two MWDSs of interest from four stations in the California Cooperative Snow Survey Network (Rattlesnake, Robinson Cow Camp, Greek Store, and Alpha) and two stations from the Snowpack Telemetry Network (SNOTEL; Central Sierra Snow Laboratory and Echo Summit; Figure 2a). Two stations, Rattlesnake and Alpha, were burned in 2021 by the Dixie and Caldor Fires, respectively, but remained functional.

To characterize the frequency of MWDSs and place recent MWDS in a climatological context, we used daily precipitation spanning 1 October 1917–15 April 2022 from the Tahoe City National Weather Service Cooperative Observer Program. MWDS were defined as consecutive periods of time with no daily precipitation exceeding 2.54 mm between 1 November and 31 March.

2.5. Weather Regimes

To provide a synoptic-planetary perspective and compare atmospheric circulation patterns during the two MWDS winters, we used the weather regime catalog of Guirguis et al. (2022), which evaluates the daily joint phase relationships between four regionally important modes of atmospheric variability (Guirguis et al., 2020). We extended this product to include the winter of 2021–2022. We focus on the days of the MWDS period (30 December–18 February) shared between the 2 years.

3. Results

3.1. Fire Activity Increased in Seasonal and Ephemeral Snow Zones

Fire detections show peaks during singular years (2008, 2018) and groups of years (2012–2016, 2020–2021; Figure 1a) across California's seasonal and ephemeral snow zones (Figure 1b). In calendar years 2020 and 2021 (2020–2021 inclusive), an abrupt increase in snow zone fire detections occurred. Approximately 50% of total 2001–2021 fire detections in seasonal snow zones and ∼35% in ephemeral snow regions occurred in 2020–2021. A factor of 9.8 increase in mean annual fire detections in the seasonal snow zone occurred in 2020–2021 compared with the 2001–2019 average. Fire activity in snow zones was widespread throughout 2001–2021 (Figure 1c), with a broad distribution of fire occurrence prior to 2020 (Figure 1d). However, very large fires including the Dixie,

Figure 2. (a) Map of stations and sample locations with fire names. (b) Zoomed-in map of Caldor Fire showing locations of snow, weather, and albedo observations, with elevation data from Abrams et al. (2020). (c) Albedo measurements from high burn severity forest during January (Caldor Fire). (d) Foreground shows burned debris and needlecast deposited onto the snow surface in moderate burn severity forest. (e) Changes in spectral snow albedo for unburned (gold), moderate burn severity (orange) and high burn severity (red) during January (Caldor), February (Creek Fire) and April (Creek Fire). Unburned data from the Caldor Fire in January were unavailable; the plot shows estimated unburned albedo using unburned data from Creek Fire adjusted upward by 0.04 to account for less grain-size growth of snow (Colbeck, 1982).

Caldor, Creek Fires, and fire complexes elsewhere during 2020–2021 clustered fire detections in snow zones (Figure 1e).

3.2. Increased Net Shortwave Radiation Following Wildfire

Snow albedo measurements in both the accumulation season (January and February) and the ablation season (April) show time-dependent decreases in snow albedo (Figure 2c). Broadband albedo decreased 25%–71%. The visible albedo (0.4–0.7 μm) decreased 17%–31% (moderate severity) and 45%–49% (high severity) compared to unburned during the accumulation season. In April, high (moderate) burn severity areas showed a visible albedo decrease of 60% (55%) compared to unburned areas. For the near-infrared (NIR; 0.7–2.5 μm), accumulation season declines ranged from 31% to 69% (moderate severity) to 47%–77% (high severity). We note that the decreased visible wavelength albedo is mainly due to light absorption by black carbon (Warren, 1982; Wiscombe & Warren, 1980), while decreased NIR albedo is likely due to a combination of increased grain size and light absorption by black carbon (Skiles & Painter, 2019; Warren, 1982; Wiscombe & Warren, 1980). Unlike dust, which has primary absorption in the visible wavelengths (He et al., 2019), black carbon is a "gray" absorber and can absorb throughout the solar spectrum. We translated our broadband snow albedo measurements to net shortwave radiation using the Beer-Lambert Law (Hellström, 2000; Monsi & Saeki, 1953) following Koshkin (2022) and Landsat-based estimates of leaf area index (LAI; a proxy for vegetation canopy) in the Caldor Fire perimeter. With a 70% reduction in Caldor LAI (Figure S1 in Supporting Information S1), post-fire net shortwave radiation increased from 6.12 W m^{-2} (unburned) to 67.68 W m^{-2} (high severity) during the MWDS. Holding canopy constant and only changing albedo, the net radiation increased to 32.35 W m^{-2} whereas if the canopy is removed, but the albedo remains constant, the net radiation increased to 9.91 W m^{-2}.

3.3. Rapid Snowmelt During a Midwinter Dry Spell Following Wildfire

The long-term median MWDS at Tahoe City is 22 days. During water year (WY) 2022, Tahoe City experienced its second-longest MWDS (46 days). Since 1917, three of the five longest MWDS occurred since WY2011, including WY2015 (third longest, 43 days), WY2022 (second longest), and the record-setting WY2012 (60 days). Although WY2013 (tied for 11th with 36 days) did not experience as prolonged of a MWDS as WY2022, the well-below average precipitation following a wet start to the WY provides an object lesson year for comparison. In both WY2013 and WY2022, heavy precipitation during October–December produced substantial early season snowpacks (338–770 mm SWE), and was followed by dry conditions (Figure 3a) and similar radiation. Compared with WY2013, 5% more accumulated solar radiation occurred during WY2022 between 28 December–18 February period at the unburned Red Baron RAWS (2b) but approximately equal radiation between 28 December–1 March (Figure S2 in Supporting Information S1).

SWE declined faster at the two burned sites, Alpha and Rattlesnake, compared to the unburned sites during WY2022's MWDS (Figure 3b). In contrast, all stations behaved similarly during the WY2013 MWDS (Figure 3c), though Rattlesnake began melting in mid-March. Compared to the date of maximum SWE, the SWE at unburned sites declined by 0%–4% in WY2013% and 0%–8% in WY2022 over the course of the dry period. During WY2013, Alpha and Rattlesnake declined by 2%–9% during the MWDS. However, in WY2022, burned stations declined 41%–45%, consistent with enhanced net shortwave radiation in burned environments (Figure 2). After a small precipitation event on 18 February 2022, snowpack continued to decline at Rattlesnake but remained consistent at Alpha before declining in late March. Compared to WY2013, snow at both Alpha and Rattlesnake disappeared earlier during WY2022 (Figures 3b and 3c).

3.4. Midwinter Dry Spell Weather Regimes

Analysis of weather regimes (WR) reveals broad similarities between WY2013 and WY2022 during the MWDS (Figures 3d and 3e) and throughout the accumulation season (Figure S3 in Supporting Information S1). The bulk of snow accumulation in December during both years was associated with WR favoring wet conditions and snowfall (Figures S3 and S4 in Supporting Information S1; Guirguis et al., 2022). Beginning in late December (WY2013) or early January (WY2022) a WR shift occurred bringing atmospheric ridging conditions over/offshore from California (Figures S3 and S4 in Supporting Information S1). Similar dry-type WRs but with varying frequencies occurred during the respective MWDS (Figures 3d and 3e). The cessation in SWE

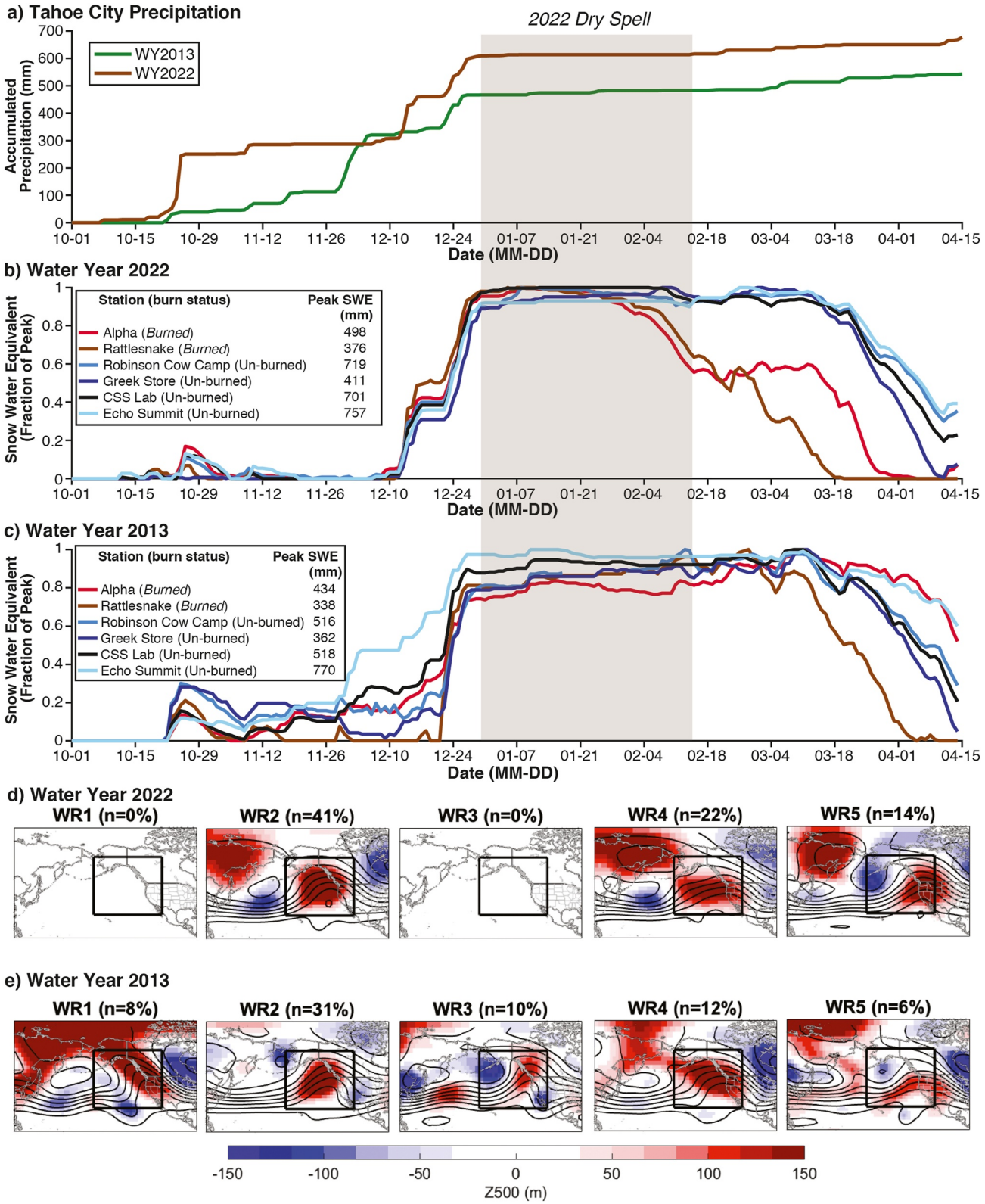

Figure 3. (a) Accumulated precipitation at Tahoe City during WY2013 and WY2022. (b) Snow water equivalent (SWE) as a fraction of peak SWE during water year (WY) 2022. (c) As in (b) but for WY2013. Primary dry weather regimes (WR) and their frequency derived from atmospheric reanalysis products (Guirguis et al., 2022) during the MWDS of 30 December–18 February of (d) WY2022, and (e) WY2013.

accumulation is associated with the onset and persistence of WRs bringing persistent high pressure leading to a MWDS (Figures 3d and 3e). High pressure patterns were more persistent in WY2022 (Figure 3d). WY2013 was more variable with short-lived weather pattern changes allowing for small snow accumulation events (Figure 4b). These events appear as intermittent breakdowns of the ridging patterns and development of patterns (e.g., WR3) producing weak onshore flow (Figure 3e).

3.5. Snow Remote Sensing Indicates Post-Fire Snowpack Decline

Despite similar conditions in snowpack at the beginning of each MWDS (Figures 3b and 3c) and generally similar meteorological conditions (Figures 3d and 3e and Figure S3 in Supporting Information S1), remote sensing shows widespread, rapid post-wildfire snowmelt throughout the accumulation and melt seasons within the Caldor Fire perimeter (Figure 4). Snow-covered area declined faster during January and February WY2022 compared to WY2013 (Figure 4a), with 50% less snow cover at the end of the WY2022 MWDS. Albedo resets following snowfall were more common in WY2013 than WY2022 (Figure 4b), with WY2022 demonstrating the lowest fire perimeter-average snow albedos on record in early February. Consistent with lower albedo (Figures 2c and 4b), melt occurred faster after storms in WY2022 compared to WY2013 (Figure 4a). Impacts within the fire perimeter are clear with over 50 fewer snow cover days by 30 April (Figure 4c), giving WY2022 the lowest snow cover days in the MODIS record. Dry conditions during November (Figure 3a) and melt-out of October snowfall (Figure 3b) contributed to the initial (1 January) lower cumulative days of snow cover in WY2022 (Figure 4c). In contrast, WY2013 was near-to-above average in terms of snow cover days until late April (Figure 4c).

Spatial comparisons for February mean snow cover fractions show WY2013 had near-to-slightly below the 2001–2022 mean, whereas WY2022 had well-below mean snow cover fractions within the Caldor Fire perimeter (and Tamarack Fire perimeter; Figures 1e, 4d, and 4e). By 1 March, snow cover days were 20–50 days below average only in the lowest elevation (western-most) regions during WY2013 whereas strong correspondence between anomalous below-mean snow cover days and the Caldor fire perimeter occur during WY2022 (Figures 4f and 4g). These differences increased as the season progressed (Figure S7 in Supporting Information S1).

4. Discussion

Wildfires in seasonal and ephemeral snow zones are expected. Our identified abrupt, near-10-fold increase in fire activity during 2020–2021 in California's snow zones relative to the previous 18 years (Figure 1) is embedded in an increasing trend in California wildfire activity (Alizadeh et al., 2021; Gleason et al., 2019). Conditions conducive to large, severe fires will increase as the climate warms (Abatzoglou & Williams, 2016; Gutierrez et al., 2021; Williams et al., 2019) and becomes more volatile (Gershunov et al., 2019). This implies future fire activity in snow zones will more frequently resemble 2020 and 2021.

Decreases in both albedo (Figures 2b–2d) and canopy (Figure S1 in Supporting Information S1) increase the net shortwave radiation and accelerate snowmelt during MWDS (Figure 3c; Gleason et al., 2013). Additional radiation reduces snow covered area (Figure 4c) directly and indirectly through positive feedbacks (Koshkin, Hatchett, & Nolin, 2022). Similar results associated with local and long-range transport and deposition of fire-generated LAPs occurs in seasonally snow-covered regions (Gleason et al., 2019; Uecker et al., 2020) and glacial environments (Aubry-Wake et al., 2022). However, these studies focused on the ablation season rather than the accumulation season. Dust deposition could further accelerate wildfire-induced midwinter melt (Huang et al., 2022). Similar to dust-on-snow (Skiles & Painter, 2019), in post-fire environments, radiative forcing-induced positive feedbacks likely occur between grain size growth, albedo decline from melt-driven LAP accumulation, and larger-scale albedo decline as the land surface becomes snow-free (Huang et al., 2022; Koshkin, Hatchett, & Nolin, 2022; Sterle et al., 2013; Warren, 1982). Despite some of the lowest midwinter albedos on record, further investigation of why our remotely sensed WY2022 albedo values did not decline to values as low as measured in-situ are warranted.

Our results indicate strong potential for enhanced post-fire midwinter melt under persistent high pressure (Figure 3d). Given the limited supply of charred debris, albedo-driven changes in net shortwave will dominate post-fire energy balance in the short-term (<10 years; Gleason et al., 2019). However, persistent canopy losses (requiring tens of years for forest canopy recovery; Bright et al., 2019) will eventually drive the post-fire snowpack energy balance.

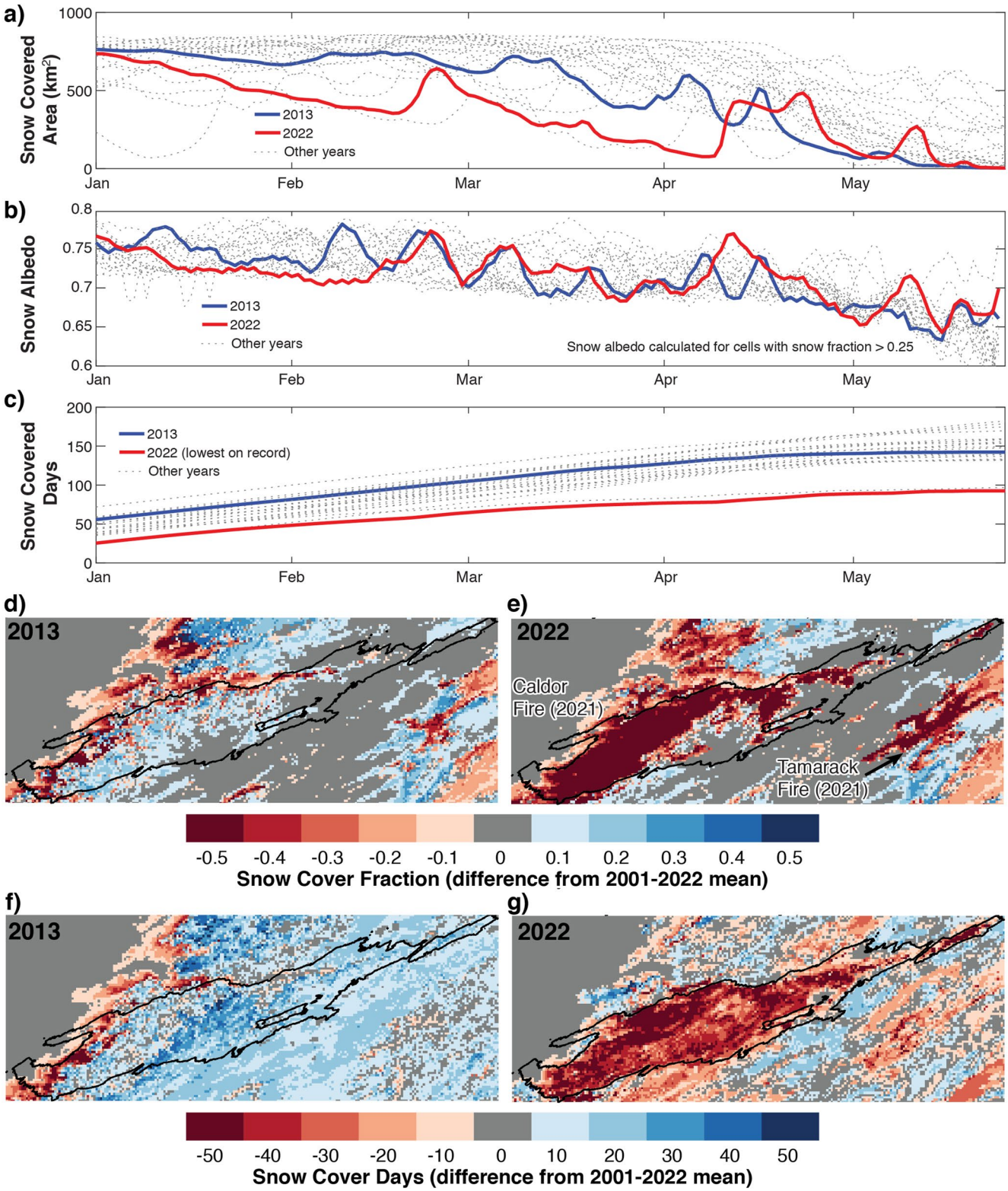

Figure 4. (a) Snow covered area (km^2) for Caldor Fire perimeter between 1 January and 31 May for water years (WYs) 2001–2022 (light dashed lines) with WY2013 and WY2022 shown as thick blue and red lines, respectively. (b) As in (a) but for snow albedo. (c) As in (a) but for snow covered days. February snow cover fractions, as differences from 2001 to 2022 mean for (d) WY2013 and (e) WY2022. End of February snow cover days (cumulative from 1 October), as differences from 2001 to 2022 mean for (f) WY2013 and (g) WY2022. Gray values indicate zeros.

Guirguis et al. (2022) found increasing frequencies of three midwinter dry patterns that parallel observed declines in California snowpack (Mote et al., 2018). These same atmospheric circulation patterns are associated with the MWDSs in WY2013 and WY2022. While both years demonstrate similar weather patterns, WY2013 had slightly more active weather compared to WY2022 (Figure S3 in Supporting Information S1). Because warmer-than-average conditions are expected during WRs 1, 4, and 5 (Guirguis et al., 2022), we also investigated the role of temperature. Tahoe City is influenced by nocturnal inversions, so we compared MWDS temperatures at the mid-slope Echo Summit SNOTEL. WY2022 experienced warmer minimum (0.5°C) and maximum (0.5°C) temperatures than WY2013, with both years observing multiple nights with minimum temperatures above freezing (Figure S5 in Supporting Information S1). Warm nights and copious solar radiation (Figures S2 and S5 in Supporting Information S1) facilitated region-wide melt, amplifying the effects of post-fire net shortwave radiation in burned areas but insufficient to drive rapid melt in unburned areas (Figures 3b and 4a). Sunny and non-freezing conditions are likely responsible for the slightly greater midwinter melting outside burned areas in WY2022 compared to WY2013, evident in areas north of the Caldor Fire (Figures 4e and 4g; Figures S6 and S7 in Supporting Information S1). These general meteorological consistencies between the years imply observed melt patterns resulted predominantly from altered land surface conditions rather than meteorological differences.

Amplified post-fire midwinter melt raises concern for hydrologic resources and hazards. Enhanced temperature- and radiation-driven midwinter melt with greater snow accumulation (Maxwell & Clair, 2019) could elevate soil moisture earlier in the season and make snowpacks more hydrologically-active (Brandt et al., 2022). Additional soil moisture increases runoff efficiency and soil pore water pressures, leading to elevated runoff during rain-on-snow events (Heggli et al., 2022) and higher probabilities for shallow landslides (Collins & Znidarcic, 2004; Iverson, 2000). Midwinter runoff affects reservoir operations as traditional regulatory frameworks may not allow for additional reservoir storage when flood risk reduction is the primary management concern (Maina & Siirila-Woodburn, 2020; Williams et al., 2022). Moreover, higher rates of sediment influx from burned areas entering reservoirs (Sankey et al., 2017; B. P. Murphy et al., 2018) reduce water quality (S. F. Murphy et al., 2012) and damage infrastructure (Randle et al., 2021).

The compounding effects of post-fire impacts on snow and MWDSs pose challenges for climate projections and operational forecasts. More frequent wildfire in snow zones and additional dry days are expected with warming (Hatchett et al., 2022; Polade et al., 2014; Westerling, 2018). Midwinter snowpack loss and early melt leads to drier late-season soil and vegetation conditions (Harpold & Molotch, 2015). Skillfully predicting WR associated with anomalous wet or dry conditions at subseasonal-to-seasonal scales provides lead-time to implement mitigation measures for altered hydrology (Guirguis et al., 2022). However, mitigation requires skillful hydrologic forecasts. If post-fire effects on snow exacerbate trends toward elevated runoff (Uzun et al., 2021; Williams et al., 2022), direct updates of snow albedo to operational hydrologic models and improved parameterizations of fire-snow relationships in Earth-system models is required (Hao et al., 2022).

5. Conclusions

We identified abrupt increases in wildfire activity in California's snow zones in 2020 and 2021 that reduced both snow albedo and canopy cover and likely accelerated snowmelt during an extended mid-winter dry spell. To enhance water-supply reliability, reduce flood hazards, and inform adaptation strategies, aspects impacted by the growing geographical overlap between wildfire and mountain snowpacks, we recommend improving process-based representation and inclusion of wildfire's impacts in the snow zone in short- and long-term operational hydrologic and Earth system models.

Data Availability Statement

MODIS fire detections are available from the NASA Fire Information for Resources Management System (https://firms.modaps.eosdis.nasa.gov/). The ASTER Global Digital Elevation Model V003 is available from the NASA EOSDIS Land Processes DAAC (https://doi.org/10.5067/ASTER/ASTGTM.003). Weather regime data (Guirguis et al., 2022) is available from the UCSD library digital collections (https://doi.org/10.6075/J089161B). The University of Arizona Snow Water Equivalent Product is available from the NASA National Snow and Ice Data Center Distributed Active Archive Center (https://doi.org/10.5067/0GGPB220EX6A). Station data is publicly available for SNOTEL stations from the United States Natural Resources Conservation Agency

(https://wcc.sc.egov.usda.gov/reportGenerator/) with RAWS data available from the Desert Research Institute (https://raws.dri.edu) and COOP data available from the Applied Climate Information System (https://www.rcc-acis.org). The MODIS data is available from the Zenodo repository: (Rittger & Hatchett, 2023; https://doi.org/10.5281/zenodo.7522988). Spectrometer data is available from the Zenodo repository (Koshkin, Nolin, & Hatchett 2022; https://doi.org/10.5281/zenodo.7545408).

Acknowledgments
BJH and AK were supported by the National Integrated Drought Information System under agreement 1332KP21DNEEN0006. AMR was funded by the U.S. Department of Energy Regional and Global Climate Modeling Program (Award Nos. DE-AC02-05CH11231 and DE-SC0016605). KG and AG were funded by the U.S. Department of the Interior via the Bureau of Reclamation (USBR-R15AC00003) and via the Southwest Climate Adaptation Science Center (G18AC00320). KR was funded by NASA Grants 80NSSC18K0427 and 80NSSC22K0929. We appreciate the thoughtful and constructive reviews from Francis Rengers and two anonymous reviewers. Any use of trade, product, or firm names is for descriptive purposes only and does not imply endorsement by the U.S. government.

References

Abatzoglou, J. T., & Williams, A. P. (2016). Impact of anthropogenic climate change on wildfire across western U.S. forests. *Proceedings of the National Academy of Sciences*, *113*(42), 11770–11775. https://doi.org/10.1073/pnas.1607171113

Abrams, M., Crippen, R., & Fujisada, H. (2020). ASTER global digital elevation model (GDEM) and ASTER global water body dataset (ASTWBD). *Remote Sensing*, *12*(7), 1156. https://doi.org/10.3390/rs12071156

Ackroyd, C., Skiles, S. M., Rittger, K., & Meyer, J. (2021). Trends in snow cover duration across river basins in high mountain Asia from daily gap-filled MODIS fractional snow covered area. *Frontiers of Earth Science*, *9*, 713145. https://doi.org/10.3389/feart.2021.713145

Alizadeh, M. R., Abatzoglou, J. T., Luce, C. H., Adamowski, J. F., Farid, A., & Sadegh, M. (2021). Warming enabled upslope advance in western U.S. forest fires. *Proceedings of the National Academy of Sciences*, *118*(22), e2009717118. https://doi.org/10.1073/pnas.2009717118

Andrews, P., & Rothermel, R. (1982). Charts for interpreting wildland fire behaviour characteristics. In *USDA forest Service general technical report, INT-131* (p. 24).

Aubry-Wake, C., Bertoncini, A., & Pomeroy, J. W. (2022). Fire and ice: The impact of wildfire-affected albedo and irradiance on glacier melt. *Earth's Future*, *10*(4), e2022EF002685. https://doi.org/10.1029/2022EF002685

Bair, E. H., Abreu Calfa, A., Rittger, K., & Dozier, J. (2018). Using machine learning for real-time estimates of snow water equivalent in the watersheds of Afghanistan. *The Cryosphere*, *12*(5), 1579–1594. https://doi.org/10.5194/tc-12-1579-2018

Bair, E. H., Rittger, K., Davis, R. E., Painter, T. H., & Dozier, J. (2016). Validating reconstruction of snow water equivalent in California's Sierra Nevada using measurements from the NASA Airborne Snow Observatory. *Water Resources Research*, *52*(11), 8437–8460. https://doi.org/10.1002/2016WR018704

Bair, E. H., Rittger, K., Skiles, S. M., & Dozier, J. (2019). An examination of snow albedo estimates from MODIS and their impact on snow water equivalent reconstruction. *Water Resources Research*, *55*(9), 7826–7842. https://doi.org/10.1029/2019WR024810

Brandt, W. T., Haleakala, K., Hatchett, B. J., & Pan, M. (2022). A review of the hydrologic response mechanisms during mountain rain-on-snow. *Frontiers of Earth Science*, *10*, 791760. https://doi.org/10.3389/feart.2022.791760

Bright, B. C., Hudak, A. T., Kennedy, R. E., Braaten, J. D., & Henareh Khalyani, A. (2019). Examining post-fire vegetation recovery with Landsat time series analysis in three western North American forest types. *Fire Ecology*, *15*(1), 8. https://doi.org/10.1186/s42408-018-0021-9

Broxton, P., Zeng, X., & Dawson, N. (2019). Daily 4 km gridded SWE and snow depth from assimilated in-situ and modeled data over the conterminous US, version 1, Boulder, Colorado USA. https://doi.org/10.5067/0GGPB220EX6A

Cheney, N. (1990). Quantifying bushfires. *Mathematical and Computer Modelling*, *13*(12), 9–15. https://doi.org/10.1016/0895-7177(90)90094-4

Colbeck, S. C. (1982). An overview of seasonal snow metamorphism. *Reviews of Geophysics*, *20*(1), 45–61. https://doi.org/10.1029/RG020i001p00045

Collins, B. D., & Znidarcic, D. (2004). Stability analyses of rainfall induced landslides. *Journal of Geotechnical and Geoenvironmental Engineering*, *130*(4), 362–372. https://doi.org/10.1061/(ASCE)1090-0241(2004)130:4(362)

Cristea, N. C., Lundquist, J. D., Loheide, S. P., II, Lowry, C. S., & Moore, C. E. (2014). Modelling how vegetation cover affects climate change impacts on streamflow timing and magnitude in the snowmelt-dominated upper Tuolumne Basin, Sierra Nevada. *Hydrological Processes*, *28*(12), 3896–3918. https://doi.org/10.1002/hyp.9909

Ebel, B. A., & Moody, J. A. (2017). Synthesis of soil-hydraulic properties and infiltration timescales in wildfire-affected soils. *Hydrological Processes*, *31*(2), 324–340. https://doi.org/10.1002/hyp.10998

Gershunov, A., Shulgina, T., Clemesha, R. E. S., Guirguis, K., Pierce, D. W., Dettinger, M. D., et al. (2019). Precipitation regime change in Western North America: The role of atmospheric rivers. *Scientific Reports*, *9*(1), 9944. https://doi.org/10.1038/s41598-019-46169-w

Gleason, K. E., McConnell, J. R., Arienzo, M. M., Chellman, N., & Calvin, W. M. (2019). Four-fold increase in solar forcing on snow in western U.S. burned forests since 1999. *Nature Communications*, *10*(1), 2026. https://doi.org/10.1038/s41467-019-09935-y

Gleason, K. E., & Nolin, A. W. (2016). Charred forests accelerate snow albedo decay: Parameterizing the post-fire radiative forcing on snow for three years following fire. *Hydrological Processes*, *30*(21), 3855–3870. https://doi.org/10.1002/hyp.10897

Gleason, K. E., Nolin, A. W., & Roth, T. R. (2013). Charred forests increase snowmelt: Effects of burned woody debris and incoming solar radiation on snow ablation. *Geophysical Research Letters*, *40*(17), 4654–4661. https://doi.org/10.1002/grl.50896

Guirguis, K., Gershunov, A., DeFlorio, M. J., Shulgina, T., Delle Monache, L., Subramanian, A. C., et al. (2020). Four atmospheric circulation regimes over the North Pacific and their relationship to California precipitation on daily to seasonal timescales. *Geophysical Research Letters*, *47*(16), e2020GL087609. https://doi.org/10.1029/2020GL087609

Guirguis, K., Gershunov, A., Hatchett, B., Shulgina, T., DeFlorio, M. J., Subramanian, A. C., et al. (2022). Winter wet–dry weather patterns driving atmospheric rivers and Santa Ana winds provide evidence for increasing wildfire hazard in California. *Climate Dynamics*. https://doi.org/10.1007/s00382-022-06361-7

Gutierrez, A. A., Hantson, S., Langenbrunner, B., Chen, B., Jin, Y., Goulden, M. L., & Randerson, J. T. (2021). Wildfire response to changing daily temperature extremes in California's Sierra Nevada. *Science Advances*, *7*(47), eabe6417. https://doi.org/10.1126/sciadv.abe6417

Hao, D., Bisht, G., He, C., Bair, E., Huang, H., Dang, C., et al. (2022). Improving snow albedo modeling in E3SM land model (version 2.0) and assessing its impacts on snow and surface fluxes over the Tibetan Plateau. *Geoscientific Model Development Discussions*, *16*, 1–31. https://doi.org/10.5194/gmd-2022-67

Harpold, A. A., & Molotch, N. P. (2015). Sensitivity of soil water availability to changing snowmelt timing in the western U.S. *Geophysical Research Letters*, *42*(19), 8011–8020. https://doi.org/10.1002/2015GL065855

Hatchett, B. (2021). Seasonal and ephemeral snowpacks of the conterminous United States. *Hydrology*, *8*(1), 32. https://doi.org/10.3390/hydrology8010032

Hatchett, B., Rhoades, A., & McEvoy, D. (2022). Decline in seasonal snow during a projected 20-year dry spell. *Hydrology*, *9*(9), 155. https://doi.org/10.3390/hydrology9090155

He, C., Liou, K.-N., Takano, Y., Chen, F., & Barlage, M. (2019). Enhanced snow absorption and albedo reduction by dust-snow internal mixing: Modeling and parameterization. *Journal of Advances in Modeling Earth Systems*, *11*(11), 3755–3776. https://doi.org/10.1029/2019MS001737

Heggli, A., Hatchett, B., Schwartz, A., Bardsley, T., & Hand, E. (2022). Toward snowpack runoff decision support. *Science*, *25*(5), 104240. https://doi.org/10.1016/j.isci.2022.104240

Hellström, R. R. (2000). Forest cover algorithms for estimating meteorological forcing in a numerical snow model. *Hydrological Processes*, *14*(18), 3239–3256. https://doi.org/10.1002/1099-1085(20001230)14:18⟨3239::AID-HYP201⟩3.0.CO;2-O

Huang, H., Qian, Y., He, C., Bair, E. H., & Rittger, K. (2022). Snow albedo feedbacks enhance snow impurity-induced radiative forcing in the Sierra Nevada. *Geophysical Research Letters*, *49*(11), e2022GL098102. https://doi.org/10.1029/2022GL098102

Immerzeel, W. W., Lutz, A. F., Andrade, M., Bahl, A., Biemans, H., Bolch, T., et al. (2020). Importance and vulnerability of the world's water towers. *Nature*, *577*(7790), 364–369. https://doi.org/10.1038/s41586-019-1822-y

Iverson, R. M. (2000). Landslide triggering by rain infiltration. *Water Resources Research*, *36*(7), 1897–1910. https://doi.org/10.1029/2000WR900090

Justice,C.,Giglio,L.,Korontzi,S.,Owens,J.,Morisette,J.,Roy,D.,etal.(2002).TheMODISfireproducts.*RemoteSensingofEnvironment*,*83*(1),244–262. (The Moderate Resolution Imaging Spectroradiometer (MODIS): a new generation of Land Surface Monitoring). https://doi.org/10.1016/S0034-4257(02)00076-7

Kaspari, S., McKenzie Skiles, S., Delaney, I., Dixon, D., & Painter, T. H. (2015). Accelerated glacier melt on Snow Dome, Mount Olympus, Washington, USA, due to deposition of black carbon and mineral dust from wildfire. *Journal of Geophysical Research: Atmospheres*, *120*(7), 2793–2807. https://doi.org/10.1002/2014JD022676

Keeley, J. (2009). Fire intensity, fire severity and burn severity: A brief review and suggested usage. *International Journal of Wildland Fire*, *18*(1), 116–126. https://doi.org/10.1071/WF07049

Key, C. H., & Benson, N. C. (2006). Landscape assessment (la). In D. C. Lutes, R. E. Keane, J. F. Caratti, C. H. Key, N. C. Benson, S. Sutherland, et al. (Eds.), *FIREMON: Fire effects monitoring and inventory system. Gen. Tech. Rep. RMRS-GTR-164-CD* (Vol. 164, p. LA-1-55). US Department of Agriculture, Forest Service, Rocky Mountain Research Station.

Koshkin, A., Nolin, A., & Hatchett, B. J. (2022). Winter season spectral snowpack albedo data for the Caldor and Creek Fires [Dataset]. Zenodo. https://doi.org/10.5281/zenodo.7545408

Koshkin, A. L. (2022). *Wildfire impacts on western United States snowpacks*. M.S. Thesis. University of Nevada.

Koshkin, A. L., Hatchett, B. J., & Nolin, A. W. (2022). Wildfire impacts on Western United States snowpack. *Frontiers in Water*, *4*, e2021WR031569. https://doi.org/10.3389/frwa.2022.971271

Lynn, E., Cuthbertson, A., He, M., Vasquez, J. P., Anderson, M., Abatzoglou, J. T., & Hatchett, B. J. (2020). Technical note: Precipitation-phase partitioning at landscape scales to regional scales. *Hydrology and Earth System Sciences*, *24*(1), 1–16. https://doi.org/10.5194/hess-24-1-2020

Maina, F. Z., & Siirila-Woodburn, E. R. (2020). Watersheds dynamics following wildfires: Nonlinear feedbacks and implications on hydrologic responses. *Hydrological Processes*, *34*(1), 33–50. https://doi.org/10.1002/hyp.13568

Maxwell, J., & Clair, S. B. S. (2019). Snowpack properties vary in response to burn severity gradients in montane forests. *Environmental Research Letters*, *14*(12), 124094. https://doi.org/10.1088/1748-9326/ab5de8

McEvoy, D. J., Hobbins, T. J., Brown, M., VanderMolen, K., Wall, T., Huntington, J. L., & Svoboda, M. (2019). Establishing relationships between drought indices and wildfire danger outputs: A test case for the California-Nevada drought early warning system. *Climate*, *7*(4), 52. https://doi.org/10.3390/cli7040052

Millar, C. I., & Stephenson, N. L. (2015). Temperate forest health in an era of emerging megadisturbance. *Science*, *349*(6250), 823–826. https://doi.org/10.1126/science.aaa9933

Moeser, C. D., Broxton, P. D., Harpold, A., & Robertson, A. (2020). Estimating the effects of forest structure changes from wildfire on snow water resources under varying meteorological conditions. *Water Resources Research*, *56*(11), e2020WR027071. https://doi.org/10.1029/2020WR027071

Monsi, M., & Saeki, T. (1953). Über den Lichtfaktor in den Pflanzengesellschaften und seine Bedeutung für die Stoffproduktion. *Japanese Journal of Botany*, *14*, 22–52.

Mote, P. W., Li, S., Lettenmaier, D. P., Xiao, M., & Engel, R. (2018). Dramatic declines in snowpack in the western US. *npj Climate and Atmospheric Science*, *1*(1), 2. https://doi.org/10.1038/s41612-018-0012-1

Murphy, B. P., Yocom, L. L., & Belmont, P. (2018). Beyond the 1984 perspective: Narrow focus on modern wildfire trends underestimates future risks to water security. *Earth's Future*, *6*(11), 1492–1497. https://doi.org/10.1029/2018EF001006

Murphy, S. F., McCleskey, R. B., & Writer, J. H. (2012). Effects of flow regime on stream turbidity and suspended solids after wildfire, Colorado Front Range. In *Wildfire and water quality—Processes, impacts, and challenges* (Vol. 354, pp. 51–58). IAHS Publication Canada.

Painter, T. H., Bryant, A. C., & Skiles, S. M. (2012). Radiative forcing by light absorbing impurities in snow from MODIS surface reflectance data. *Geophysical Research Letters*, *39*(17), 17502. https://doi.org/10.1029/2012GL052457

Painter, T. H., Rittger, K., McKenzie, C., Slaughter, P., Davis, R. E., & Dozier, J. (2009). Retrieval of subpixel snow covered area, grain size, and albedo from MODIS. *Remote Sensing of Environment*, *113*(4), 868–879. https://doi.org/10.1016/j.rse.2009.01.001

Parks, S. A., & Abatzoglou, J. T. (2020). Warmer and drier fire seasons contribute to increases in area burned at high severity in Western US forests from 1985 to 2017. *Geophysical Research Letters*, *47*(22), e2020GL089858. https://doi.org/10.1029/2020GL089858

Petersky, R., & Harpold, A. (2018). Now you see it, now you don't: A case study of ephemeral snowpacks and soil moisture response in the great basin, USA. *Hydrology and Earth System Sciences*, *22*(9), 4891–4906. https://doi.org/10.5194/hess-22-4891-2018

Polade, S. D., Pierce, D. W., Cayan, D. R., Gershunov, A., & Dettinger, M. D. (2014). The key role of dry days in changing regional climate and precipitation regimes. *Scientific Reports*, *4*(1), 4364. https://doi.org/10.1038/srep04364

Randle, T. J., Morris, G. L., Tullos, D. D., Weirich, F. H., Kondolf, G. M., Moriasi, D. N., et al. (2021). Sustaining United States reservoir storage capacity: Need for a new paradigm. *Journal of Hydrology*, *602*, 126686. https://doi.org/10.1016/j.jhydrol.2021.126686

Rittger, K., Bair, E. H., Kahl, A., & Dozier, J. (2016). Spatial estimates of snow water equivalent from reconstruction. *Advances in Water Resources*, *94*, 345–363. https://doi.org/10.1016/j.advwatres.2016.05.015

Rittger, K., & Hatchett, B. J. (2023). Spatially and temporally complete snow cover percent, snow albedo, and snow cover duration for the Caldor Fire from SCAG and DRFS (Snow Today v003) [Dataset]. Zenodo. https://doi.org/10.5281/zenodo.7522988

Rittger, K., Painter, T. H., & Dozier, J. (2013). Assessment of methods for mapping snow cover from modis. *Advances in Water Resources*, *51*, 367–380. https://doi.org/10.1016/j.advwatres.2012.03.002

Rittger, K., Raleigh, M. S., Dozier, J., Hill, A. F., Lutz, J. A., & Painter, T. H. (2020). Canopy adjustment and improved cloud detection for remotely sensed snow cover mapping. *Water Resources Research*, *56*(6), e2019WR024914. https://doi.org/10.1029/2019WR024914

Sankey, J. B., Kreitler, J., Hawbaker, T. J., McVay, J. L., Miller, M. E., Mueller, E. R., et al. (2017). Climate, wildfire, and erosion ensemble foretells more sediment in western USA watersheds. *Geophysical Research Letters*, *44*(17), 8884–8892. https://doi.org/10.1002/2017GL073979

Sarangi, C., Qian, Y., Rittger, K., Bormann, K. J., Liu, Y., Wang, H., et al. (2019). Impact of light-absorbing particles on snow albedo darkening and associated radiative forcing over high-mountain Asia: High-resolution WRF-chem modeling and new satellite observations. *Atmospheric Chemistry and Physics*, *19*(10), 7105–7128. https://doi.org/10.5194/acp-19-7105-2019

Sarangi, C., Qian, Y., Rittger, K., Ruby Leung, L., Chand, D., Bormann, K. J., & Painter, T. H. (2020). Dust dominates high-altitude snow darkening and melt over high-mountain Asia. *Nature Climate Change*, *10*(11), 1045–1051. https://doi.org/10.1038/s41558-020-00909-3

Siirila-Woodburn, E., Rhoades, A., Hatchett, B., Huning, L., Szinai, J., Tague, C., et al. (2021). Evidence of a low-to-no snow future and its impacts on water resources in the western United States. *Nature Reviews Earth & Environment*, *2*(11), 800–819. https://doi.org/10.1038/s43017-021-00219-y

Skiles, S. M., Flanner, M., Cook, J. M., Dumont, M., & Painter, T. H. (2018). Radiative forcing by light-absorbing particles in snow. *Nature Climate Change*, *8*(11), 964–971. https://doi.org/10.1038/s41558-018-0296-5

Skiles, S. M., & Painter, T. H. (2019). Toward understanding direct absorption and grain size feedbacks by dust radiative forcing in snow with coupled snow physical and radiative transfer modeling. *Water Resources Research*, *55*(8), 7362–7378. https://doi.org/10.1029/2018WR024573

Sterle, K. M., McConnell, J. R., Dozier, J., Edwards, R., & Flanner, M. G. (2013). Retention and radiative forcing of black carbon in eastern Sierra Nevada snow. *The Cryosphere*, *7*(1), 365–374. https://doi.org/10.5194/tc-7-365-2013

Stevens, J. T. (2017). Scale-dependent effects of post-fire canopy cover on snowpack depth in montane coniferous forests. *Ecological Applications*, *27*(6), 1888–1900. https://doi.org/10.1002/eap.1575

Uecker, T. M., Kaspari, S. D., Musselman, K. N., & Skiles, S. M. (2020). The post-wildfire impact of burn severity and age on black carbon snow deposition and implications for snow water resources, cascade range, Washington. *Journal of Hydrometeorology*, *21*(8), 1777–1792. https://doi.org/10.1175/JHM-D-20-0010.1

Uzun, S., Tanir, T., Coelho, G. D. A., Souza de Lima, A. D., Cassalho, F., & Ferreira, C. M. (2021). Changes in snowmelt runoff timing in the contiguous United States. *Hydrological Processes*, *35*(11), e14430. https://doi.org/10.1002/hyp.14430

Warren, S. G. (1982). Optical properties of snow. *Reviews of Geophysics*, *20*(1), 67–89. https://doi.org/10.1029/RG020i001p00067

Westerling, A. L. (2018). Wildfire simulations for California's fourth climate change assessment: Projecting changes in extreme wildfire events with a warming climate. In *California's fourth climate change assessment (technical report no. CCCA4-CEC-2018-014)*. California Energy Commission.

Williams, A. P., Abatzoglou, J. T., Gershunov, A., Guzman-Morales, J., Bishop, D. A., Balch, J. K., & Lettenmaier, D. P. (2019). Observed impacts of anthropogenic climate change on wildfire in California. *Earth's Future*, *7*(8), 892–910. https://doi.org/10.1029/2019EF001210

Williams, A. P., Livneh, B., McKinnon, K. A., Hansen, W. D., Mankin, J. S., Cook, B. I., et al. (2022). Growing impact of wildfire on western U.S. water supply. *Proceedings of the National Academy of Sciences*, *119*(10), e2114069119. https://doi.org/10.1073/pnas.2114069119

Wilson, A. C., Nolin, A. W., & Bladon, K. D. (2021). Assessing the role of snow cover for post-wildfire revegetation across the Pacific Northwest. *Journal of Geophysical Research: Biogeosciences*, *126*(11), e2021JG006465. https://doi.org/10.1029/2021JG006465

Wiscombe, W. J., & Warren, S. G. (1980). A model for the spectral albedo of snow. I: Pure snow. *Journal of the Atmospheric Sciences*, *37*(12), 2712–2733. https://doi.org/10.1175/1520-0469(1980)037⟨2712:AMFTSA⟩2.0.CO;2

Zeng, X., Broxton, P., & Dawson, N. (2018). Snowpack change from 1982 to 2016 over conterminous United States. *Geophysical Research Letters*, *45*(23), 12940–12947. https://doi.org/10.1029/2018GL079621